Boron doped diamond ultramicroelectrodes: A generic platform for sensing single nanoparticle electrocatalytic collisions

ARTICLE *in* CHEMICAL COMMUNICATIONS · MAY 2013

Impact Factor: 6.83 · DOI: 10.1039/c3cc42915f · Source: PubMed

6 AUTHORS, INCLUDING:

David Wakerley
University of Cambridge
6 PUBLICATIONS **45** CITATIONS
SEE PROFILE

Laura A Hutton
Element Six
11 PUBLICATIONS **238** CITATIONS
SEE PROFILE

Julie V Macpherson
The University of Warwick
175 PUBLICATIONS **5,614** CITATIONS
SEE PROFILE

ChemComm

RSC Publishing

COMMUNICATION

View Article Online
View Journal | View Issue

Boron doped diamond ultramicroelectrodes: a generic platform for sensing single nanoparticle electrocatalytic collisions†

Cite this: *Chem. Commun.*, 2013, **49**, 5657

Received 19th April 2013,
Accepted 13th May 2013

DOI: 10.1039/c3cc42915f

www.rsc.org/chemcomm

David Wakerley,‡[a] Aleix G. Güell,‡[a] Laura A. Hutton,[a] Thomas S. Miller,[a] Allen J. Bard[b] and Julie V. Macpherson*[a]

Boron doped diamond (BDD) disk ultramicroelectrodes have been used to sense single nanoparticle (NP) electrocatalytic collision events. BDD serves as an excellent support electrode due to its electrocatalytic inactivity and low background currents and thus can be used to detect the electroactivity of a wide range of colliding NPs, with high sensitivity. In particular, single NP collisions for hydrazine oxidation at Au and Pt NPs were shown to be markedly different.

In order to study single nanoparticle (NP) electrocatalytic collision events the choice of electrode material, at which the NPs collide, is crucial.[1,2] Ideally, the electrode should be electrocatalytically inert towards the redox reaction of interest such that it only serves as an electrical contact for the colliding NP. In this way, it is possible to measure the minute change in current arising from the electrocatalytic redox process associated with a single NP colliding with the electrode surface.

Electrode materials such as gold (Au)[3] and platinum (Pt),[4] have been employed as the electrode support, however as both display electrocatalytic activity it is only possible to use certain electrode and NP combinations. For example, for the study of hydrazine (HZ) electro-oxidation at individual Pt NPs, an Au support electrode can be employed, however, for the same redox process Au NPs cannot be used with a Pt electrode,[4] due to HZ electro-oxidation occurring at more negative potentials at a Pt electrode compared to Au.[3]

It is well-documented that boron doped diamond (BDD) electrodes are electrocatalytically inactive, provided no non-diamond-like impurities are present. This most likely arises from the sp^3 surface termination which does not favour molecular adsorption, unlike transition metals which offer d orbitals. Additionally, unlike metal electrodes, BDD does not undergo surface oxidations or reductions, resulting in reduced background currents and a low double layer capacitance ($\ll 10\ \mu F\ cm^{-2}$).[5]

In order to investigate individual NP electrocatalytic collision events, ultramicroelectrodes (UMEs) are required to minimise the number of collisions per unit time. Although cone-shaped BDD UMEs exist, where the BDD has been grown directly onto sharpened metallic wires,[6,7] these are far from ideal due to the large area exposed, non co-planar surface and the rough surface. Arrays of UME disks have been fabricated from both polycrystalline and nanocrystalline BDD, but never at the single electrode scale, as required herein.

In this communication, we report the fabrication of single co-planar disk-shaped BDD UMEs, of typical diameters in the range 50–100 μm, for use in the investigation of HZ oxidation at single Au and Pt NPs. The BDD is laser cut to reveal a "top hat" structure as shown in Fig. 1(a). The BDD is sealed in insulating

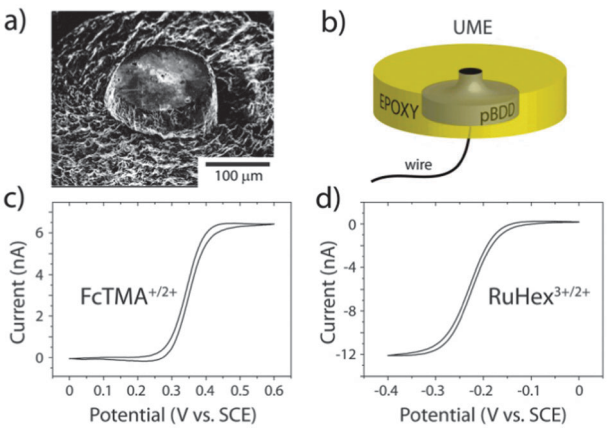

Fig. 1 (a) Electron microscopy image of the 'top hat' structure. (b) A schematic of the BDD UME. (c) and (d) CVs recorded at a 60 μm diameter disk BDD UME in 1 mM $FcTMA^+$ and 1.3 mM $(Ru(NH_3)_6)^{3+}$ respectively, at 10 mV s^{-1} in 0.1 M KCl.

[a] *Department of Chemistry, University of Warwick, Coventry, CV4 7AL, UK. E-mail: j.macpherson@warwick.ac.uk; Fax: +44 (0)2476 524112; Tel: +44 (0)2476 573886*

[b] *Department of Chemistry and Biochemistry, The University of Texas, Austin, USA. Fax: +1 512 471 0088; Tel: +1 512 471 3761*

† Electronic supplementary information (ESI) available: (I) Fabrication of the BDD UMEs. (II) Electrodepositions of Pt NPs and Au NPs on BDD UME. (III) Synthesis and characterisation of NPs. (IV) Sensing nanoparticles collisions. (V) Au NP collisions. See DOI: 10.1039/c3cc42915f

‡ DW and AGG contributed equally to this work.

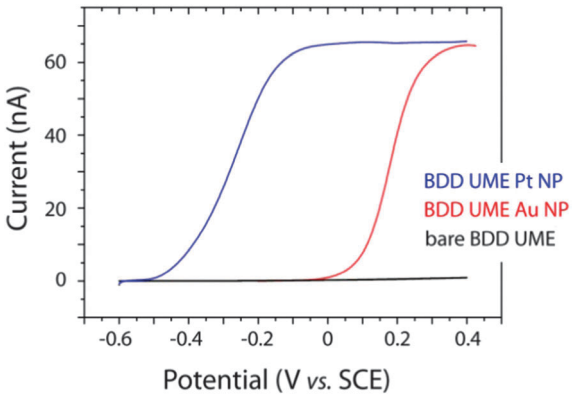

Fig. 2 Typical CVs for HZ oxidation at a 90 μm BDD disk UME (black line), in the presence of Pt NPs (blue line) and Au NPs (red line) recorded at 10 mV s^{-1}. The analyte solution contained 0.5 mM hydrazine and 50 mM phosphate buffer solution (pH = 7.2).

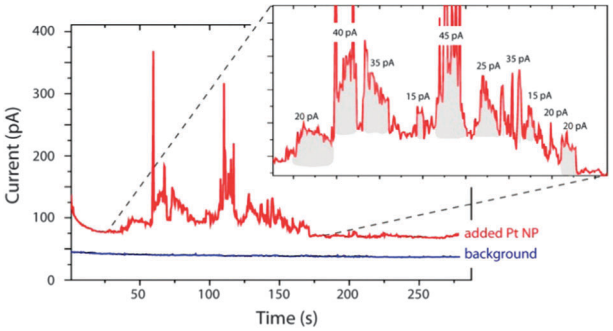

Fig. 3 A current–time trace for a 50 μm BDD UME in 10 mM hydrazine and 50 mM phosphate buffer solution with (red) and without (blue) Pt NPs. The electrode was held at +0.2 V *vs.* SCE and the trace was carried out at 1×10^{-4} s time intervals.

epoxy and then polished carefully to reveal a co-planar structure (Fig. 1(b)). Further experimental details are found in Section I (ESI†).

To verify the electrochemical response of the BDD disk UMEs, two, fast, one electron transfer, outer sphere, reversible mediators were chosen, (ferrocenylmethyl) trimethylammonium hexafluorophosphate ($FcTMA^{+/2+}$) and ruthenium hexaamine ($Ru(NH_3)_6^{3+/2+}$) with very different formal potentials (E^o values). Fig. 1(c) and (d) show typical cyclic voltammograms (CVs) acquired at a BDD disk UME of diameter ~60 μm, measured optically. A difference in the $\frac{1}{4}$-wave and $\frac{3}{4}$-wave potential, $E_{1/4} - E_{3/4}$, of ~57 mV is found for both couples indicative of reversible heterogeneous electron transfer (HET). The steady-state currents for diffusion limited HET to a co-planar disk UME are also in good agreement with those predicted theoretically, assuming diffusion coefficients, $D(Ru(NH_3)_6^{3+})$ and $D(FcTMA^+)$ of 8.8×10^{-6} cm^2 s^{-1} and 6×10^{-6} cm^2 s^{-1} respectively.[8]

HZ oxidation, an inner sphere HET reaction, was examined electrochemically at a bare BDD disk UME (black line) and a BDD UME decorated with electrodeposited Pt (blue line) and Au NPs (red line),[9–11] Fig. 2; details on NP electrodeposition are provided in ESI† Section II. The NPs were electrodeposited at a high enough density to ensure complete diffusional overlap during HZ oxidation. For BDD, in the potential region examined, the electrode is clearly electrochemically inactive towards HZ oxidation. In contrast, in the presence of both Au and Pt NPs, steady state limiting currents are observed, with HET for HZ oxidation at the Pt NPs ($E_{1/2} \approx -0.3$ V *vs.* SCE) occurring at more negative potentials than for Au NPs ($E_{1/2} \approx 0.2$ V *vs.* SCE). Assuming that for HZ oxidation the number of transferred electrons is 4, and the electrode diameter is 90 μm, we obtain a D_{HZ} of 5.5×10^{-6} cm^2 s^{-1}, which lies within the range of reported values.[12] Fig. 2 thus clearly demonstrates that using a BDD UME it is possible to electrochemically detect HZ oxidation at *both* Pt and Au NPs.

Au and Pt NP colloidal solutions were synthesized *via* chemical reduction of the appropriate metallic salt in aqueous solution, in the presence of sodium citrate acting as a capping agent;[13,14] further information is provided in ESI† Section III. NP shape and size were characterised by means of transmission electron microscopy (TEM) and atomic force microscopy (AFM); (ESI,† Section III).

For all experiments, the BDD electrode was held at a potential where the HZ oxidation reaction occurred under diffusion-controlled conditions. From Fig. 2, for Pt NP collisions the electrode was held at 0.2 V *vs.* SCE, whilst for Au NPs a potential of 0.4 V *vs.* SCE was applied. A full description of the experimental set-up and NP injection procedure is given in ESI† Section IV.

Fig. 3 shows typical current transients recorded at a 50 μm BDD UME before and after the injection of Pt NPs, ranging in diameter, 2–6 nm. In the absence of NPs, the background current trace remains below 50 pA, and appears smooth and featureless. Compared to Au UME studies of HZ oxidation at single NPs using similar applied potentials and solution conditions, the background currents recorded here are typically five times smaller, even though the electrode used herein is five times larger in diameter.[3] This exemplifies the low background currents of high quality BDD electrodes. In the presence of Pt NPs, distinct changes in the current, or 'current events', are observed as a result of NPs interacting directly with the electrode surface.

The current events that arise depend on how the NP interacts with the electrode surface. Previous research by Bard and co-workers has shown that NP collisions fall generally into either one of two categories, staircases or blips.[1] The former is a result of single NPs permanently sticking to the electrode surface creating a stepwise accumulation of steady state current, whilst the latter occurs when NPs collide but do not stick to the surface, creating current spikes in the time response. The current–time (*i*–*t*) response for HZ oxidation due to Pt NPs colliding with the BDD electrode interestingly shows both current blips and steps (Fig. 3), although the blip behaviour is more dominant. The current steps (as shown on Fig. 3) at some point always fall back down again, indicating that although the NP sticks to the surface, it does not remain permanently stuck. Alternatively, the decrease in current could also indicate blockage or ''deactivation'' of the NP surface.[3]

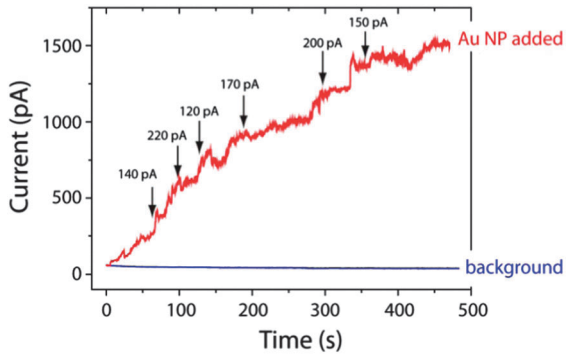

Fig. 4 An *i–t* trace of a 50 μm BDD UME in 10 mM hydrazine and 50 mM phosphate buffer solution with Au NPs. The electrode was held at +0.4 V *vs.* SCE and the trace was carried out at 1×10^{-4} s time intervals.

The standalone steps are characterised by an initial current spike, attributed to the first contact of the NP to the electrode, followed by a diffusion-controlled current whilst the NP remain attached or within a tunnelling distance to the electrode. This current can be predicted using eqn (1) which describes radial diffusion to a sphere on a plane:[15]

$$i_{ss} = 4\pi(\ln 2)Fn_oC_oD_or_{NP} \quad (1)$$

where F is the Faraday constant, D_o is the diffusion coefficient of the redox species, C_o is the concentration of the redox species and r_{NP} is the NP radius. The 2–6 nm diameter Pt NPs should, in agreement with eqn (1), produce currents in the range 30–80 pA, which agrees well with the currents seen in Fig. 3.

The same configuration was employed to detect the oxidation of HZ at Au NPs colliding with the BDD UME. The resulting *i–t* traces (Fig. 4 and ESI,† Section V) before and after adding Au NPs clearly show an increase in the measured current, assigned to the electrocatalytic oxidation of HZ at Au NPs landing on the BDD surface. However, in stark contrast to the Pt NPs, the current events arising from Au NP collisions more closely resemble current staircases, suggesting that the Au NPs are sticking permanently to the electrode surface.[16] AFM and TEM characterisation revealed Au NP diameters in the range 9–16 nm (ESI,† Section III), resulting in diffusion limiting currents between 90–160 pA (eqn (1)), which match well with the current step sizes observed in the transients recorded. Observing single Au NP electrocatalytic collision events for HZ oxidation is challenging as most electrode materials are not electrochemically inert enough in the potential region of interest to function effectively as a support.

To rule out the effect of NP size contributing to the different current events observed for the Pt NPs and Au NPs, further Au NP collision experiments were carried out but with smaller NPs. The response was equivalent, exhibiting staircase collisions, but with smaller current magnitudes (Section V, ESI†).

The question arises as to why Pt and Au NPs show very different *i–t* traces. The BDD surface is polycrystalline, has been polished to ~nm roughness and is oxygen terminated (hydrophilic). The metal NPs are ligand stabilised with strongly solvated negatively charged citrate ions (pH = 7.2). At the potentials applied (0.2 V *vs.* SCE for Pt NPs and 0.4 V *vs.* SCE for Au NPs) the surface termination of the BDD electrode is unlikely to differ; strong oxidising or reducing electrode potentials are typically required to change surface functionality.[17] Moreover, similar *i–t* traces are obtained for Pt NPs when the UME is held at +0.4 V (data not shown), indicating that more positive potentials do not favour NP sticking events.[3] Thus it appears it is the chemical identity of the metal NP which controls the observed behaviour. This is currently the subject of further work.

In summary, by using electrocatalytically inert co-planar disk BDD UMEs it is possible to study a wide range of single NP electrocatalytic collision events, using the same substrate electrode. Furthermore BDD offers the opportunity to study many different metal NPs for the same electrocatalytic process. Here, using a BDD UME it has been possible to study the oxidation characteristics of HZ at both Pt NP and Au NPs colliding with the same support electrode, for the first time.

AGG would like to thank EPSRC (EP/H023909/1) for funding. We all thank Element Six Ltd (Ascot, UK) for provision of the BDD. Equipment used in this research was obtained through Science City (AM2), with support from Advantage West Midlands.

Notes and references

1 S. J. Kwon, H. Zhou, F.-R. F. Fan, V. Vorobyev, B. Zhang and A. J. Bard, *Phys. Chem. Chem. Phys.*, 2011, **13**, 5394–5402.
2 S. J. Kwon, F.-R. F. Fan and A. J. Bard, *J. Am. Chem. Soc.*, 2010, **132**, 13165–13167.
3 X. Xiao, F.-R. F. Fan, J. Zhou and A. J. Bard, *J. Am. Chem. Soc.*, 2008, **130**, 16669–16677.
4 H. Zhou, F.-R. F. Fan and A. J. Bard, *J. Phys. Chem. Lett.*, 2010, **1**, 2671–2674.
5 H. V. Patten, L. A. Hutton, K. E. Meadows, J. G. Iacobini, D. Battistel, K. McKelvey, A. W. Colburn, M. E. Newton, J. V. Macpherson and P. R. Unwin, *Angew. Chem., Int. Ed.*, 2012, **51**, 7002–7006.
6 J. S. Foord, J. Hu and K. B. Holt, *Phys. Status Solidi A*, 2007, **204**, 2940–2944.
7 K. B. Holt, J. Hu and J. S. Foord, *Anal. Chem.*, 2007, **79**, 2556–2561.
8 A. J. Bard and L. R. Faulkner, *Electrochemical Methods – Fundamentals and Applications*, 2nd edn, John Wiley & Sons, INC., New York, US, 2001.
9 P. V. Dudin, P. R. Unwin and J. V. Macpherson, *J. Phys. Chem. C*, 2010, **114**, 13241–13248.
10 T. A. Ivandini, D. Yamada, T. Watanabe, H. Matsuura, N. Nakano, A. Fujishima and Y. Einaga, *J. Electroanal. Chem.*, 2010, **645**, 58–63.
11 L. Hutton, M. E. Newton, P. R. Unwin and J. V. Macpherson, *Anal. Chem.*, 2009, **81**, 1023–1032.
12 S. E. F. Kleijn, S. C. S. Lai, T. S. Miller, A. I. Yanson, M. T. M. Koper and P. R. Unwin, *J. Am. Chem. Soc.*, 2012, **134**, 18558–18561.
13 N. R. Jana, L. Gearheart and C. J. Murphy, *J. Phys. Chem. B*, 2001, **105**, 4065–4067.
14 J. Yang, J. Y. Lee and H.-P. Too, *Anal. Chim. Acta*, 2006, **571**, 206–210.
15 X. Xiao and A. J. Bard, *J. Am. Chem. Soc.*, 2007, **129**, 9610–9612.
16 R.-H. Tian, T. N. Rao, Y. Einaga and J.-f. Zhi, *Chem. Mater.*, 2006, **18**, 939–945.
17 T. N. Rao, I. Yagi, T. Miwa, D. A. Tryk and A. Fujishima, *Anal. Chem.*, 1999, **71**, 2506–2511.